

Avoiding Big Integers: Parallel Multimodular Algebraic Verification of Arithmetic Circuits

Clemens Hofstadler¹[0000-0002-3025-0604], Daniela Kaufmann²[0000-0002-5645-0292], and Chen Chen³[0009-0007-8825-6260]

¹ Johannes Kepler University, Linz, Austria clemens.hofstadler@jku.at

² TU Wien, Austria daniela.kaufmann@tuwien.ac.at

³ Hong Kong University of Science and Technology (Guangzhou), China
cchen099@connect.hkust-gz.edu.cn

Abstract. Word-level verification of arithmetic circuits with large operands typically relies on arbitrary-precision arithmetic, which can lead to significant computational overhead as word sizes grow. In this paper, we present a hybrid algebraic verification technique based on polynomial reasoning that combines linear and nonlinear rewriting. Our approach relies on multimodular reasoning using homomorphic images, where computations are performed in parallel modulo different primes, thereby avoiding any large-integer arithmetic. We implement the proposed method in the verification tool TALISMAN2.0 and evaluate it on a suite of multiplier benchmarks. Our results show that hybrid multimodular reasoning significantly improves upon existing approaches.

Keywords: Computer Algebra · Hardware Verification · Homomorphic Images · Linear Extractions · Guess and Prove

1 Introduction

Word-level reasoning using computer algebra has proven to be an effective approach for the formal verification of arithmetic circuits, especially for circuits encoding nonlinear operations, such as multiplier and divider circuits [13, 19, 21, 26, 27], as it avoids the combinatorial blow-up caused by bit-blasting. In this line of work, circuits are translated into systems of polynomial equations whose solutions characterize all valid circuit behaviors. Verification then reduces to proving that a given specification polynomial is implied by the circuit encoding.

A major practical limitation of existing word-level algebraic reasoning approaches is their reliance on large-integer arithmetic. For arithmetic circuits with word sizes of 64 bits and beyond, the resulting polynomial systems contain coefficients whose bit-widths exceed native machine word sizes by orders of magnitude. For instance, the specification of 64-bit multipliers contains coefficients up to 2^{127} . As a result, state-of-the-art reasoning tools typically depend on arbitrary-precision arithmetic, e.g., the implementations of [12, 20, 25, 26] all rely on the GMP library [9], which incurs significant computational overhead and limits scalability in practice.

In this paper, we address this limitation by introducing a verification framework based on *parallel multimodular reasoning*. Our approach avoids large-integer arithmetic entirely by computing *homomorphic images* of the polynomial system modulo multiple machine-word-sized prime numbers. Rather than reasoning over \mathbb{Z} or \mathbb{Q} , all computations are carried out modulo those primes in parallel, ensuring that coefficients remain within machine word sizes throughout the verification process. The Chinese remainder theorem ensures the correctness of this approach, provided that sufficiently many primes are used (Theorem 1). While homomorphic images are a classical tool in computer algebra, see e.g., [8, Ch. 5], to the best of our knowledge this is the first work to employ them for word-level circuit verification. In Section 4, we present our multimodular approach in detail and prove its correctness.

To exploit multimodular reasoning effectively, we combine it with a *hybrid rewriting framework* that integrates both linear and nonlinear algebraic reasoning (see Section 5). Linearization-based techniques [13,19] extract linear relations from the algebraic encoding of the circuit to enable a fast linear rewriting of the previously linearized circuit specification. We build upon the guess-and-prove strategy presented in [13]. The core idea is to sample valid assignments for extracted subcircuits, from which linear relations are guessed using linear algebra. The correctness of these guesses is proved using satisfiability (SAT) solving. In this paper, we significantly improve, parallelize, and adapt this approach to our multimodular setting (Section 5.1). In particular, we apply a structure-aware subcircuit selection, weighted sampling for more targeted assignments, and dedicated linear algebra routines to better handle a large number of samples. All of these optimizations significantly improve the guess-and-prove strategy.

When linear reasoning becomes computationally infeasible due to the size of the selected subcircuit, our framework switches to nonlinear rewriting, using the nonlinear circuit encoding to continue rewriting the specification until completion (Section 5.2). This combination yields the efficiency of linearization together with the robustness of nonlinear reasoning. Additionally, this procedure allows us to always produce counterexamples in case of faulty circuits, which is not always possible in pure linear approaches.

We implement the proposed approach in our novel verification tool TALISMAN2.0 [14]⁴, which we discuss in detail in Section 5, and evaluate it on a suite of multiplier benchmarks (Section 6). The results demonstrate that parallel multimodular reasoning combining linear and nonlinear rewriting is able to efficiently solve a large set of benchmarks while remaining robust.

2 Preliminaries

In Section 2.1, we review fundamental concepts from polynomial algebra that are required throughout this work. For a more comprehensive introduction, we refer to the standard textbooks [6,7]. In Section 2.2, we recall And-Inverter Graphs (AIGs) and describe how they can be represented by polynomial encodings.

⁴ We will move the source code to a permanent online repository upon acceptance.

2.1 Algebra

Let $X = \{x_1, \dots, x_n\}$ be a finite set of indeterminates and let R be a commutative ring with unity. A *monomial* (in X) is a product of the form $x_1^{\alpha_1} \dots x_n^{\alpha_n}$, where $\alpha_1, \dots, \alpha_n \in \mathbb{N}$. The set of all monomials in X is denoted by $[X]$.

A *polynomial* f (over R) is a finite R -linear combination of monomials, i.e., $f = c_1 m_1 + \dots + c_s m_s$, with *coefficients* $c_1, \dots, c_s \in R$ and monomials $m_1, \dots, m_s \in [X]$. The product $c_i m_i$ is called a *term*. The set of all polynomials is denoted by $R[X] = R[x_1, \dots, x_n]$.

The *degree* $\deg(m)$ of a monomial $m = x_1^{\alpha_1} \dots x_n^{\alpha_n} \in [X]$ is defined as the sum of its exponents, that is, $\deg(m) = \alpha_1 + \dots + \alpha_n$. A polynomial f is called *linear* if every monomial m in f has $\deg(m) \leq 1$, otherwise f is called *nonlinear*.

Many algebraic operations require an ordering of monomials. A *monomial order* is a total order \prec on $[X]$ such that $1 \prec m$ for all $m \neq 1$, and $m_1 \prec m_2$ implies $mm_1 \prec mm_2$ for all $m, m_1, m_2 \in [X]$. Typical examples are the *lexicographic order*, which compares exponent vectors componentwise, and the *degree lexicographic order*, which first compares degrees and breaks ties lexicographically. An order is *degree-compatible* if smaller degree implies smaller order.

With respect to a fixed monomial order, every nonzero polynomial $f \in R[X]$ has a unique maximal monomial, called its *leading monomial* and denoted by $\text{lm}(f)$. The product of this monomial with its coefficient is called the *leading term*, denoted by $\text{lt}(f)$.

A nonempty subset $I \subseteq R[X]$ is an *ideal* if it is closed under addition, i.e., $f + g \in I$ for all $f, g \in I$, and under multiplication by arbitrary polynomials, i.e., $hf \in I$ for all $f \in I$ and $h \in R[X]$. A finite set of polynomials $F = \{f_1, \dots, f_r\} \subseteq R[X]$ can be interpreted as a system of equations $f_1 = \dots = f_r = 0$. The set of all polynomials h whose equation $h = 0$ can be derived algebraically from this system forms an ideal, denoted by $\langle F \rangle$. It is given explicitly by $\langle F \rangle = \{h_1 f_1 + \dots + h_r f_r \mid h_1, \dots, h_r \in R[X]\}$.

2.2 And-Inverter Graphs and their Polynomial Encodings

An *And-Inverter Graph* (AIG) [28] is a directed acyclic graph representing a Boolean circuit C . Internal nodes correspond to logical conjunctions, while edge annotations encode negation. Primary inputs correspond to Boolean variables.

A *specification* of an AIG is a polynomial $\mathcal{S} \in R[X]$, where R is a chosen coefficient domain (typically \mathbb{Z}) and X contains all input, gate, and output variables of the circuit. The specification relates the outputs of the circuit to its primary inputs. Although AIGs operate on Boolean signals, the specification is not restricted to the Boolean ring $\mathbb{B}[X]$. For instance, the specification of multipliers with inputs $a_{n-1}, \dots, a_0, b_{n-1}, \dots, b_0$ and outputs s_{2n-1}, \dots, s_0 can be represented as $\sum_{i=0}^{2n-1} 2^i s_i - (\sum_{i=0}^{n-1} 2^i a_i) \cdot (\sum_{i=0}^{n-1} 2^i b_i)$ over $\mathbb{Z}[X]$ or $\mathbb{Q}[X]$.

To relate the behavior of gates in the circuit to polynomial equations, we map $\top \mapsto 1$ and $\perp \mapsto 0$, yielding the correspondences $x \wedge y \simeq xy$ and $\neg x \simeq 1 - x$ between logic and algebra. Based on these relations, we define the following *gate polynomials* for gates in a circuit.

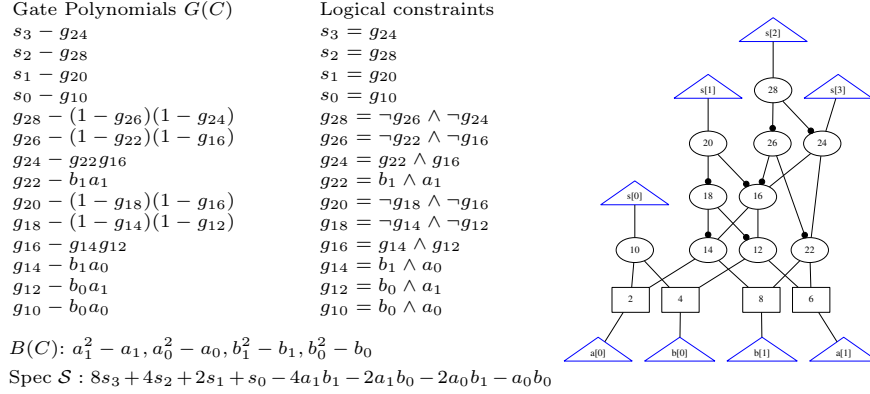


Fig. 1. AIG and polynomial encoding of a 2-bit multiplier.

Definition 1. The gate polynomial of an AIG node g with inputs x, y is:

Logical constraint	\Rightarrow	Gate polynomial
$g = x \wedge y$	\Rightarrow	$g - xy$
$g = \neg x \wedge y$	\Rightarrow	$g - (1 - x)y$
$g = x \wedge \neg y$	\Rightarrow	$g - x(1 - y)$
$g = \neg x \wedge \neg y$	\Rightarrow	$g - (1 - x)(1 - y)$

We denote by $G(C) \subseteq R[X]$ the set of all gate polynomials of a circuit C .

To enforce Boolean semantics when working over coefficient domains $R \neq \mathbb{B}$, we introduce *Boolean value polynomials*. For each primary input x_i of the AIG, we define the constraint $x_i^2 - x_i = 0$. We denote the set of all such polynomials by $B(C)$. Boolean constraints propagate through the circuit, and it therefore suffices to introduce Boolean value polynomials only for the primary inputs [22].

Example 1. Figure 1 shows an AIG representing a 2-bit multiplier and its corresponding polynomial encoding. We denote the primary inputs by a_0, a_1, b_0, b_1 and outputs by s_0, s_1, s_2, s_3 . The internal nodes are denoted by g_i , where i corresponds to the respective AIG node. The specification \mathcal{S} expresses that the weighted sum of output bits (= output bit-vector) is equal to the product of the weighted sum of input bits (= input bit-vectors).

To relate a circuit to its specification, we recall the notion of models from [21]. First, recall that a (*Boolean*) *assignment* is a function $\varphi: X \rightarrow \{0, 1\} \subseteq R$ that maps the variables in X to the values 0 and 1. Any assignment φ can be extended to an evaluation of polynomials by substituting $\varphi(x)$ for each variable $x \in X$. For a polynomial $p \in R[X]$, we denote the evaluation under φ by $\varphi(p) \in R$.

Definition 2. Let $P \subseteq R[X]$ be a set of polynomials. A (*Boolean*) assignment φ is a model of P (over R) if $\varphi(p) = 0$ for all $p \in P$. Moreover, for $q \in R[X]$, we write $P \models_R q$ if every model for P is also a model for $\{q\}$, i.e., whenever $\varphi(p) = 0$ for all $p \in P$, then also $\varphi(q) = 0$.

We say that a circuit C *fulfills* a specification \mathcal{S} (over R) if $G(C) \models_R \mathcal{S}$. Note that, since we consider only Boolean assignments, this is equivalent to $G(C) \cup B(C) \models_R \mathcal{S}$. By [23, Thm. 2,3], this holds if and only if the specification polynomial \mathcal{S} lies in the ideal $\langle G(C) \cup B(C) \rangle$. Hence, correctness of C can be verified algebraically by checking whether $\mathcal{S} \in \langle G(C) \cup B(C) \rangle$. Classically, this computation is performed over $R = \mathbb{Z}$ (or $R = \mathbb{Q}$ when a field is required). In Section 4, we present a multimodular approach that reduces verification over \mathbb{Z} to verification over sufficiently many finite rings \mathbb{Z}_{m_i} .

3 Related Work

In principle, the ideal membership $\mathcal{S} \stackrel{?}{\in} \langle G(C) \cup B(C) \rangle$ is decidable using Gröbner basis theory [5]. To this end, the set $G(C) \cup B(C)$ needs to be transformed into a Gröbner basis, which can be of double exponential complexity in the number of variables in the worst case [31]. However, if a lexicographic monomial order is chosen such that variables follow the reverse topological order of the circuit, the set $G(C) \cup B(C)$ already forms a Gröbner basis [23]. Thus, correctness of the circuit can be decided by computing the remainder of \mathcal{S} under multivariate polynomial division with respect to $G(C) \cup B(C)$, see [6, Ch. 2.3]. We refer to this approach as *nonlinear rewriting*.

For multiplier verification, nonlinear rewriting with respect to a lexicographic order is known to suffer from severe *monomial blow-up*. Since the leading term of gate polynomials typically has lower degree than the remaining terms (cf. Definition 1), the degree of intermediate results may increase substantially. This frequently produces intermediate results with millions of monomials [29] and drastically slows down computations.

To mitigate this effect, several advanced rewriting engines have been proposed in recent years. Early work employed dedicated preprocessing and incremental reasoning [21], where syntactically identified parts of the multiplier are rewritten using SAT solving prior to applying a column-wise verification algorithm [20]. Subsequent refinements eliminated the reliance on an external SAT solver by introducing a syntactic algebraic encoding that incorporates literal polarities [18]. However, the dependence on syntactic heuristics remains a major limitation of these approaches, since such heuristics are often not robust for unseen circuit architectures, such as those generated by logic synthesis.

Orthogonal to this line of work, dynamic rewriting approaches determine the rewrite order on the fly and backtrack if intermediate results exceed a predefined threshold [30]. This idea was further extended by incorporating literal polarities into the encoding in later work [26]. While this approach is more robust across different circuit architectures, it remains infeasible for certain multiplier designs that require rewriting long standalone carry chains.

Recent approaches depart from the lexicographic ordering and instead employ *degree-compatible* orderings to prevent degree growth during rewriting [13,19]. By linearizing the specification, rewriting is restricted to linear polynomials, which avoids the monomial blow-up. We refer to this approach as *linear rewriting*.

Linear rewriting comes at the cost of having to extract suitable linear relations from the circuit. To address this, on-the-fly techniques have been proposed that identify subcircuits and compute Gröbner bases locally to derive the required linear relations [19], as well as approaches based on algebraic transformations and guess-and-prove techniques [13]. Among these, the guess-and-prove approach has shown particular promise, as it can handle comparatively large subcircuits (> 1000 nodes). In this technique, a subcircuit is selected and valid assignments for that subcircuit are generated. Linear algebra is then used to derive candidate linear relations (“guesses”), which subsequently need to be proven, for instance, using SAT solving. If a candidate relation is invalid, a counterexample returned by the SAT solver can be used to refine the guess. If no suitable relation is found, the subcircuit is expanded and the process is repeated, see [13, Sec. 3.2, 4] for a more in-depth discussion.

Despite its effectiveness, the guess-and-prove approach has notable limitations. First, performance degrades significantly once the extracted subcircuit exceeds a certain size (> 5000 nodes). Second, due to large coefficients in guessed polynomials, the SAT-based proofs can become infeasible in practice, as the coefficients of the derived polynomials must be encoded at the bit level.

Our work addresses these shortcomings by applying linear rewriting via the guess-and-prove approach using *multimodular* computations, which impose explicit bounds on coefficients. Moreover, whenever linear extraction becomes too costly we propose to switch to nonlinear rewriting, thereby combining the strengths of both paradigms in a hybrid approach.

4 Multimodular Verification via Homomorphic Images

Algebraic word-level verification of arithmetic circuits with real-world input sizes of 64 bits and beyond faces a fundamental scalability bottleneck: intermediate coefficients arising during symbolic reasoning may become extremely large. As a consequence, verification procedures must rely on arbitrary-precision arithmetic, which is significantly slower than native machine-word operations that can exploit fast hardware arithmetic.

Such *expression swell* is a well-known challenge in computer algebra. Classic examples include linear system solving and Gröbner basis computations over the integers or rationals. To address this issue, computer algebra systems often employ *homomorphic images* [1, 4, 15, 34]. The central idea of homomorphic images is to map computations from an unbounded domain, such as \mathbb{Z} or \mathbb{Q} , into finite algebraic structures, typically into \mathbb{Z}_m , the integers modulo m , where all elements have a fixed-size representation and no expression swell can occur. Typically, m is chosen to be a prime number, such that \mathbb{Z}_m is a finite field, ensuring desirable algebraic properties for reasoning and computation.

Concretely, in our setting this idea translates into the following multimodular verification strategy: Instead of verifying that a circuit C fulfills a specification \mathcal{S} over \mathbb{Z} , we perform the verification modulo several integers m_1, \dots, m_k (typically primes). Working in \mathbb{Z}_{m_i} ensures that coefficients remain bounded, and when the

moduli m_i are chosen to fit within machine words, we can rely on fast native arithmetic. The Chinese remainder theorem [8, Ch. 5.4] ensures the correctness of the circuit over the integers, provided that sufficiently many moduli are used.

To formally justify this approach, we first observe that the set of models of a circuit does not depend on whether computations are carried out over the integers or modulo an integer $m \geq 2$.

Lemma 1. *Let C be an AIG and $m \geq 2$ be a positive integer. An assignment φ is a model of $G(C)$ over \mathbb{Z} if and only if it is a model of $G(C)$ over \mathbb{Z}_m .*

Proof. If $\varphi(p) = 0$ over \mathbb{Z} , then clearly $\varphi(p) \equiv 0 \pmod{m}$. Thus, any model over \mathbb{Z} is also a model over \mathbb{Z}_m . Conversely, assume that φ is not a model of $G(C)$ over \mathbb{Z} , i.e., there exists $p \in G(C)$ such that $\varphi(p) \neq 0$. Since p is a gate polynomial, $\varphi(p) \in \{-1, 1\}$. For $m \geq 2$, both values remain nonzero modulo m , implying that $\varphi(p) \not\equiv 0 \pmod{m}$. So, φ is also not a model of $G(C)$ over \mathbb{Z}_m .

Using Lemma 1, we can now prove our main result, which reduces verification over \mathbb{Z} to verification over finitely many modular domains. The maximum below ranges over all Boolean assignments φ .

Theorem 1. *Let C be an AIG and let $\mathcal{S} \in \mathbb{Z}[X]$ be a specification of C . Let $M = \max_{\varphi} |\varphi(\mathcal{S})|$ and let $m_1, \dots, m_k \in \mathbb{N} \setminus \{0, 1\}$ be pairwise coprime positive integers such that $\prod_{i=1}^k m_i > M$. Then*

$$G(C) \models_{\mathbb{Z}} \mathcal{S} \quad \text{iff} \quad \forall i \in \{1, \dots, k\} : G(C) \models_{\mathbb{Z}_{m_i}} \mathcal{S}.$$

Proof. First, assume that $G(C) \models_{\mathbb{Z}} \mathcal{S}$ holds. Let $i \in \{1, \dots, k\}$ be arbitrary and let φ be a model of $G(C)$ over \mathbb{Z}_{m_i} . By Lemma 1, φ is also a model of $G(C)$ over \mathbb{Z} . Thus, by assumption $\varphi(\mathcal{S}) = 0$ over \mathbb{Z} , which implies $\varphi(\mathcal{S}) \equiv 0 \pmod{m_i}$, showing that φ is also a model of \mathcal{S} over \mathbb{Z}_{m_i} .

Conversely, assume that $G(C) \models_{\mathbb{Z}_{m_i}} \mathcal{S}$ holds for all $i = 1, \dots, k$. Let φ be a model of $G(C)$ over \mathbb{Z} . Again by Lemma 1, φ is also a model of $G(C)$ over each \mathbb{Z}_{m_i} . Hence, $\varphi(\mathcal{S}) \equiv 0 \pmod{m_i}$ for all i by assumption. By the Chinese remainder theorem [8, Cor. 5.3], this implies $\varphi(\mathcal{S}) \equiv 0 \pmod{\prod_{i=1}^k m_i}$. Since $|\varphi(\mathcal{S})| \leq M < \prod_{i=1}^k m_i$, we have $\varphi(\mathcal{S}) = 0$ over \mathbb{Z} , showing that φ is also a model of \mathcal{S} over \mathbb{Z} .

Theorem 1 establishes the correctness of the multimodular verification approach, but it is deliberately agnostic about how the modular verifications of $G(C) \models_{\mathbb{Z}_{m_i}} \mathcal{S}$ are performed. In particular, this could be done by purely algebraic methods, but also using SAT-based reasoning, or any combination thereof. In the following Section 5, we will discuss how to perform the modular verification using our hybrid algebraic reasoning approach.

In practice, we typically choose the moduli m_i to be prime numbers, so that each \mathbb{Z}_{m_i} forms a finite field. This choice simplifies subsequent computations that rely on field properties. By using word-sized primes, all coefficients fit into native machine words, avoiding arbitrary-precision arithmetic altogether. In particular, as witnessed by implementations of other multimodular algorithms [11,32], it can

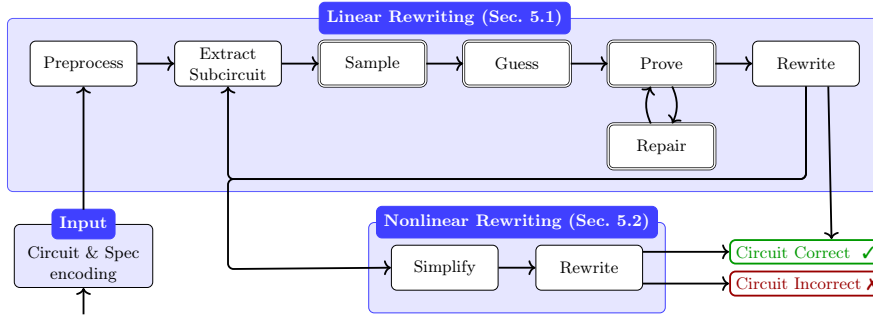


Fig. 2. Overview of the TALISMAN2.0 workflow. Double-edged boxes are computations that are run in parallel in TALISMAN2.0.

be beneficial to use 32-bit (resp. 16-bit) prime moduli while storing intermediate results in 64-bit (resp. 32-bit) (unsigned) integers. This way several arithmetic operations can be accumulated before applying a modular reduction, thereby reducing the number of expensive modulo operations.

The required number of moduli depends on an upper bound for the evaluation of the specification \mathcal{S} on all Boolean assignments φ . For example, if C implements an n -bit signed or unsigned multiplier, then $\max_{\varphi} |\varphi(\mathcal{S})| < 2^{2n}$ [21]. Consequently, for 64-bit multipliers, five 32-bit primes would suffice to meet the condition of Theorem 1. Since the verification tasks for different moduli are completely independent, they can be run in parallel, yielding near-linear speedups on modern multicore machines.

Finally, we note that the multimodular approach also supports the computation of *witnesses* of faulty circuits. By Lemma 1, any counterexample discovered during verification over a modulus \mathbb{Z}_{m_i} , that is, any model of $G(C)$ that violates \mathcal{S} modulo m_i , also forms a valid counterexample over \mathbb{Z} , and thus directly witnesses incorrect circuit behavior.

5 Hybrid Algebraic Circuit Verification

In the following, we combine the complementary strengths of linear and nonlinear rewriting in a hybrid algebraic verification framework that also makes use of the multimodular approach presented in Section 4. We also discuss implementation details of this hybrid approach in our tool TALISMAN2.0 [14] that targets verification of multiplier circuits.

The overall workflow is shown in Figure 2. Given an input AIG C , let X be the set of all input, output and internal gate variables of C . We encode the gate constraints $G(C)$ and the Boolean value polynomials $B(C)$ as described in Section 2.2. A given specification $\mathcal{S} \in \mathbb{Z}[X]$ is linearized using extension variables [13, 19]: for every nonlinear monomial m in \mathcal{S} , we introduce a new variable $v \notin X$ that acts as a placeholder. The corresponding constraints $E(C) = \{v - m \mid m \in \mathcal{S} \wedge \deg(m) > 1 \wedge v \notin X\}$ are added to the circuit encoding $G(C) \cup B(C) \cup E(C)$.

Verification then proceeds in two phases. We first apply linear rewriting as long as linear relations can be derived efficiently. Once this becomes ineffective, we switch to nonlinear rewriting. Crucially, both phases are executed over multiple prime fields using homomorphic images, ensuring that all arithmetic remains word-sized and that candidate relations can be validated efficiently. The internal structure of both phases is explained in the following sections.

5.1 Linear Rewriting

Linear rewriting aims to simplify the specification polynomial by iteratively deriving and applying linear relations implied by the circuit. After encoding and linearizing the specification, we first perform a preprocessing step to identify recurring arithmetic structures that induce linear constraints. The resulting relations are collected for subsequent use in rewriting.

The main procedure then iteratively considers the current leading monomial of the specification polynomial. To determine the leading monomial we use a reverse topological ordering of the variables. If a previously derived linear relation is applicable, it is used to rewrite the monomial. Otherwise, we select a suitable subcircuit and guess a candidate linear relation suggested by its structure. The guessed relation is then formally proved correct with respect to the circuit semantics before it is applied for rewriting. If no suitable relation can be found efficiently, we fall back to nonlinear rewriting.

Preprocessing. Many linear relations in arithmetic circuits originate from small building blocks such as half adders (HA) or full adders (FA). For example, a FA with inputs x, y, z , sum s , and carry c satisfies the linear relation $2c + s - x - y - z = 0$. Our first goal is to identify all half and full adders in the AIG. Instead of relying on syntactic pattern matching, which may be obscured by synthesis, we detect arithmetic structure semantically using cut enumeration (up to three leaves) and local truth tables, which we have implemented in our own modified version of ABC [2]. For each detected HA/FA, the corresponding linear polynomial is constructed and cached for use during linear rewriting.

Beyond local half and full adders, verification based on linear rewriting also requires us to identify higher-level adder blocks that are used to sum bit-vectors, such as the final-stage adder (FSA) in multipliers. Since the linear relations of the FSA generally depend on its global structure, it is necessary to identify a subcircuit that captures the FSA in its entirety. During preprocessing using ABC, we aim to find a subcircuit that approximates the FSA by traversing the circuit backwards from the outputs until reaching previously detected HA/FA blocks, which form a structural boundary between the FSA and the remaining circuit. Deriving a topological closure ensures that the resulting boundary forms a valid cut. Since the input size of the FSA easily exceeds 64 nodes, we do not attempt to derive its linear relations using truth tables as we did for FA/HA. Instead, they are derived later in the guess-and-prove phase, where we treat the FSA as a single extracted subcircuit. Hence, this approximation may safely over-approximate the FSA.

Extract Subcircuit. During rewriting, we consider the leading monomial of the current specification. If a cached linear polynomial with matching leading monomial exists, we immediately apply it for a rewrite step. Otherwise, we attempt to derive such a relation via guess-and-prove on a suitable subcircuit. If the corresponding gate is part of the FSA approximation, we consider the entire FSA subcircuit. If not, we extract a depth-bounded subcircuit rooted at that gate. Notably, all nodes whose children are contained in the subcircuit will also be added to the subcircuit. Hence, the subcircuit may have more than one output node. If no suitable linear relation is found, we increase the depth bound and repeat the procedure with an enlarged subcircuit. In the worst case we would need to increase the subcircuit until it covers the whole circuit.

Sample. To infer candidate relations in a suitable subcircuit, we generate samples of assignments to the subcircuit variables. In our previous work [13], we relied on uniform sampling over the inputs, with the values of internal gate variables being determined by propagation through the circuit structure. While this approach is simple and fast, it can miss rare but semantically relevant behaviors. This limitation becomes apparent in subcircuits that include long sequences of AND gates. The output of an n -ary AND gate $x = x_0 \wedge \dots \wedge x_{n-1}$ is 1 if and only if all n inputs x_i are set to 1. Under uniform input sampling, this assignment occurs with probability 2^{-n} . As a result, the guessing procedure most likely observes only assignments for which $x = 0$, leading to incorrect guesses.

To address this issue, we replace uniform input sampling with the weighted uniform-like sampler CMSGEN [10]. Unlike uniform sampling over subcircuit inputs, CMSGEN constructs uniformly sampled assignments over *all* circuit variables. It does this incrementally, by propagating implications induced by the current assignment and by learning from conflicts encountered during this process. This significantly improves coverage of rare behaviors as the results in Section 6 show. We typically generate three times as many samples as the subcircuit size.

Guess. After sampling, the candidate linear relations modulo a prime p are computed by solving the linear system $Ax = 0$ over \mathbb{Z}_p , where the columns of the matrix A correspond to variables and the rows to samples, cf. [13, Alg. 2].

In TALISMAN2.0, we now apply a trick to speed up this linear algebra step. The matrices arising in our context have a special structure: they contain only entries from $\{0, 1\}$ and they have a lot more rows than columns. We exploit this structure by solving the system $(BA)x = 0$ instead of $Ax = 0$, where B is a randomly chosen $\{0, 1\}$ -matrix. Since both A and B have entries in $\{0, 1\}$, the product BA can be computed efficiently (over \mathbb{Z}_p) using bitwise operations. By choosing B to have fewer rows than A , the resulting system becomes smaller and thus easier to solve. In our implementation, B is chosen so that BA is a square matrix. The resulting (square) systems are solved using the number theory library FLINT [35]. Every solution of the original system $Ax = 0$ is also a solution of $(BA)x = 0$, and if B is chosen randomly, then the two solution spaces coincide with high probability. Any spurious solutions introduced by the projec-

tion would be eliminated during the subsequent prove step. In our experiments, we never encountered such spurious solutions.

Prove & Repair. We prove the correctness of the linear guesses using SAT solving. To establish that a linear guess f is correct over \mathbb{Z}_p , we must show that for all models φ of the extracted subcircuit, $\varphi(f) \equiv 0 \pmod p$. We translate each gate of the extracted subcircuit into conjunctive normal form (CNF) using Tseitin transformation, and encode $f \neq 0$ in CNF using PBLIB [33]. We then prove that the formula is unsatisfiable using the SAT solver CADIICAL [3].

However, encoding $f \neq 0$ alone is actually too weak in our modular setting, since f may evaluate to a non-zero multiple of p . Therefore, whenever the SAT solver returns a satisfying assignment φ , we explicitly check whether $\varphi(f) \equiv 0 \pmod p$. If this is the case, the assignment is excluded from the search space and the SAT call is repeated. We have experimented with directly encoding $f \neq 0 \wedge f \neq p \wedge \dots \wedge f \neq lp$ for a suitable upper bound l . However, this caused a significant overhead, even for $l = 2$. Additionally, we also experimented with mixed-integer programming, but did not observe any significant difference.

Only if we obtain a satisfying assignment with $\varphi(f) \not\equiv 0 \pmod p$ do we accept it as a witness that the guess f is incorrect. We add φ as a new sample to the matrix BA in order to repair the linear guesses and re-solve the updated linear system $(BA)x = 0$. The resulting refined guesses must then be verified again for correctness.

Rewrite. Once all correct guesses have been collected, we use them to rewrite the specification as far as possible. In TALISMAN2.0, we perform rewriting steps modulo different primes simultaneously by representing each coefficient of a multimodular polynomial f as a vector, where the i th entry stores the coefficient of f modulo the i th prime. In this way, monomials have to be stored only once and coefficient arithmetic can be efficiently vectorized using SIMD instructions on modern CPUs.

Example 2. Suppose we want to rewrite the specification $\mathcal{S} = -5x + 4b + 3a$ using the linear polynomial $f = 3x + b - a$ over the three prime moduli $\mathcal{M} = (7, 11, 13)$. We first represent \mathcal{S} componentwise as $\mathcal{S} = (2, 6, 8)x + (4, 4, 4)b + (3, 3, 3)a$, since $-5 \equiv (2, 6, 8) \pmod{\mathcal{M}}$. Say x is the leading monomial of \mathcal{S} and f . Then we first normalize f by inverting its x -coefficient modulo each prime. Multiplying f componentwise by $(5, 4, 9)$ yields $f' = (1, 1, 1)x + (5, 4, 9)b + (2, 7, 4)a$. Finally, we compute the following difference to cancel the x -term from \mathcal{S} :

$$\mathcal{S} - (2, 6, 8) \cdot f' \equiv (1, 2, 10)b + (6, 5, 10)a \pmod{\mathcal{M}}.$$

If the result of such a linear rewriting step is zero, the circuit satisfies the specification and the procedure terminates. Otherwise, we consider the leading monomial of the simplified specification and start the next iteration of the linear rewriting loop.

If we fail to retrieve a linear relation whose leading monomial matches that of the specification, we increase the depth of the subcircuit to be extracted. To prevent the subcircuit from growing excessively, we switch to nonlinear rewriting

if no suitable linear relation is found after increasing the subcircuit depth a fixed number of times. In TALISMAN2.0, we set this threshold to three.

Parallellization. A key property of our multimodular framework is that computations for different prime moduli are independent. Although this would allow the entire workflow in Figure 2 to be executed in parallel, such a coarse-grained strategy would duplicate substantial work, since several phases (e.g., preprocessing, subcircuit extraction, and sampling) are identical across primes. Hence, we apply a more fine-grained parallelization scheme. Circuit encoding, preprocessing, and subcircuit extraction are done in serial and shared across primes, while the guess, prove, and repair steps are parallelized across moduli, with each thread handling one prime. Sampling is parallelized as well, but independently of the primes. Here we use multiple threads to generate samples for the same subcircuit and aggregate them for guessing. Linear and nonlinear rewriting are executed serially, as further parallelization did not yield any speedups.

5.2 Nonlinear Rewriting

Once we switch from linear to nonlinear rewriting, we fix a lexicographic monomial order that orders the variables following a reverse topological order of the circuit, starting from the output variables and progressing toward the inputs. Under this ordering, each gate polynomial has a leading monomial consisting of a unique variable. This implies that $G(C) \cup B(C)$ forms a Gröbner basis [22].

Simplify. We first simplify the AIG to reduce the number of rewriting steps. To this end, we eliminate intermediate nodes that have single fanouts. Specifically, if a node g only has one parent, we directly substitute the gate constraint of g into that of its parent. We repeat this process until no such nodes remain. The gate polynomials of the rewritten AIG still form a Gröbner basis [22].

Rewrite. We iteratively rewrite the specification polynomial using the simplified gate polynomials, thereby computing the unique normal form modulo the circuit ideal. The fact that $G(C) \cup B(C)$ forms a Gröbner basis establishes the soundness and completeness of nonlinear rewriting for deciding ideal membership. If the normal form of \mathcal{S} is the zero polynomial, then the circuit fulfills the specification and is therefore correct.

Otherwise, $\mathcal{S} \notin \langle G(C) \cup B(C) \rangle$. In this case, the normal form consists only of primary inputs of the AIG. A counterexample can therefore be extracted by choosing an input assignment for which the normal form does not evaluate to zero. Deriving counterexamples is not immediately possible in purely linear rewriting approaches [13, 19], as the normal form with respect to a degree-compatible order may still contain internal circuit variables.

Nonlinear rewriting steps are performed analogously to the linear case by representing coefficients modulo different primes by coefficient vectors (cf. Example 2).

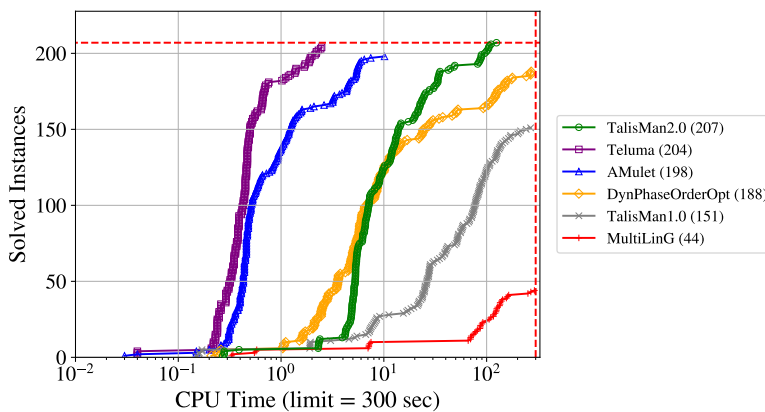


Fig. 3. Comparison of TALISMAN2.0 and related work. For each tool the number of solved instances is added in parentheses.

6 Experiments

We have implemented the presented hybrid multimodular approach in our tool called TALISMAN2.0, which acts as an improved successor of TALISMAN1 [13]. In the following, we evaluate TALISMAN2.0 and compare it to related work [13, 18–20, 26] using a total of 207 *correct* integer multiplier benchmarks.

We consider two types of benchmarks: *structured circuits*, where the components of a multiplier (partial product generation (PPG), partial product accumulation (PPA), and the final stage adder (FSA)) are clearly separable, and *synthesized circuits*, where gates are merged and rewritten to optimize the circuit, blurring component boundaries and complicating direct verification. We consider the following sets:

1. *Structured aoki-multipliers* [17]: This set of 64-bit multipliers is generated by combining different architectures for PPG, PPA, and FSA (see Appendix A) yielding 192 structured multiplier architectures.
2. *Synthesized ABC-multipliers* [2]: We generate 32-, 64-, 128-bit multipliers of type *sp-ar-rc* and optimize them with ABC using four standard synthesis scripts (resyn, resyn2, resyn3, dc2) and a complex optimization script⁵. These 15 optimized benchmarks showcase the robustness of our approach.

In our experiments, we use primes of approximately 16 bits, which provide a good trade-off between keeping the number of required moduli small and enabling efficient coefficient encoding in the SAT solver. Verifying 64-bit multipliers requires 8 such primes, while 128-bit multipliers require 16. All parallel computations use as many threads as we have primes.

The experiments were run on dual-socket AMD EPYC 7313 @3.7GHz machines running Ubuntu 24.04. Reported times are rounded wall-clock seconds.

⁵

`-c "logic; mfs2 -W 20; ps; mfs; st; ps; dc2 -1; ps; resub -1 -K 16 -N 3 -w 100; ps; logic; mfs2 -W 20; ps; mfs; st; ps; iresyn -1; ps; resyn; ps; resyn2; ps; resyn3; ps; dc2 -1; ps;"`

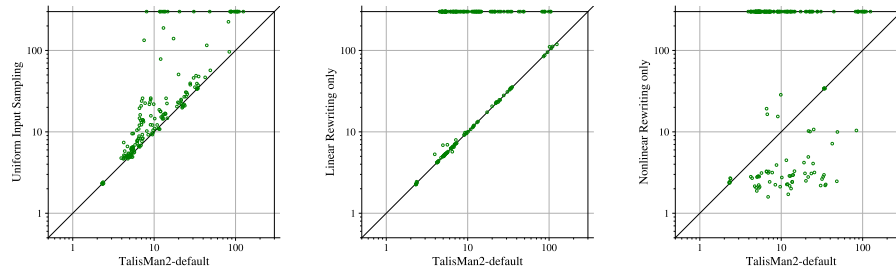


Fig. 4. Comparing the default setting when either uniform input sampling (left), only linear rewriting (middle), or only nonlinear rewriting is used (right).

The time limit was 300s and the memory limit was 32 GB to ensure sufficient resources for all tools. Notably, TALISMAN2.0 itself only required at most 5 GB.

In our first evaluation, we compare TALISMAN2.0 against tools from related work: TALISMAN1 [12,13] and MULTILING [19], both of which also apply linear rewriting. In addition, we consider DYNPHASEORDEROPT [26], AMULET2 [20, 21], and TELUMA [18], all of which use nonlinear rewriting based on a lexicographic monomial order. Figure 3 summarizes the comparison. Our main observations are:

- TALISMAN2.0 is the only tool that successfully solves all benchmarks. Increasing the time limit did not yield more successful runs for the other tools.
- AMULET2 and TELUMA solve the complete aoki benchmark set but fail on some of the synthesized ABC benchmarks. This supports our claim that their syntactic heuristics do not generalize well.
- DYNPHASEORDEROPT solves all 15 synthesized ABC benchmarks, but only 173 out of 192 aoki benchmarks. Notably, among the 19 benchmarks it fails on, 14 contain a carry-lookahead adder (cl) as FSA, indicating that this structure is hard for purely nonlinear rewriting approaches.

We highlight the runtimes of the different phases of TALISMAN2.0 from Figure 2 in Table 1. A complete table is contained in Appendix B. Notably, we only had to enter the repair phase in 36 out of 207 benchmarks. In all other cases the guesses were immediately correct. Almost all of those benchmarks have either a carry look-ahead (cl) or a conditional sum adder (cn) as the FSA.

To assess the contribution of individual components of TALISMAN2.0, we conducted an ablation study in which selected improvements were disabled. The results are shown in Figure 4. When disabling CMSGEN-based sampling and instead using uniform input sampling as in TALISMAN1 (left plot), TALISMAN2.0 fails to solve 24 benchmarks and exhibits increased runtimes on almost all remaining instances. Restricting the approach to linear rewriting only (middle plot) reduces the number of solved benchmarks to 98. Conversely, when only nonlinear rewriting is applied (right plot), 79 benchmarks can be solved; however, within this subset, TALISMAN2.0 is faster than the hybrid configuration in 63 cases, indicating that nonlinear rewriting is particularly effective on selected instances but lacks overall robustness when used in isolation.

Name	TALISMAN2.0 — Phase Times (s)									
	Total	Linear							Nonlinear	
		Prepr.	Extract	Sample	Guess*	Prove*	Repair*	Rewrite	Simplify	Rewrite
abc64-cmp	2.3	2.1	<0.05	<0.05	<0.05	<0.05	-	<0.05	-	-
bp-ar-cl	44.0	1.4	0.7	0.9	9.7	26.6	3.0	0.1	<0.05	0.2
bp-ba-cn	42.0	1.6	<0.05	2.3	23.0	3.6	5.3	<0.05	4.8	0.4
bp-bd-cl	86.2	1.4	0.9	1.6	21.6	50.1	8.3	0.2	<0.05	0.2
bp-cn-cs	13.5	1.5	<0.05	1.4	7.9	1.6	-	<0.05	0.2	0.4
bp-ct-hc	9.0	0.9	2.1	0.2	3.9	1.1	-	0.1	<0.05	0.2
bp-dt-lf	7.1	1.3	0.5	0.2	3.3	1.3	-	0.1	<0.05	0.2
bp-wt-rc	4.8	1.4	0.5	0.1	1.1	1.2	-	0.1	<0.05	0.2
sp-ar-cl	19.7	2.2	0.1	0.4	3.1	12.6	0.6	0.1	-	-
sp-ba-cn	48.6	2.7	0.1	2.8	25.0	7.1	2.8	<0.05	6.7	0.3
sp-bd-cl	88.1	2.3	0.3	1.6	19.8	54.4	7.0	0.2	-	-
sp-cn-cs	21.4	2.7	<0.05	1.3	7.9	1.8	-	<0.05	0.3	6.8
sp-ct-hc	11.9	1.6	4.2	0.2	4.1	1.3	-	0.2	-	-
sp-dt-lf	6.8	2.1	<0.05	0.2	2.8	1.4	-	0.1	-	-
sp-wt-rc	5.0	2.3	<0.05	0.2	0.9	1.4	-	0.1	-	-

Table 1. Per-phase runtime (rounded to tenths of seconds) of TALISMAN2.0. In columns marked with ‘*’ we report the average time per prime modulus. Entries ‘-’ indicate that this phase was not entered.

We evaluated the impact of replacing our custom linear algebra routines entirely by FLINT, which increases the overall runtime by 34% on average. We also investigated whether using (pseudo) Mersenne primes, i.e., primes of the form $2^k - c$ with small c , improves performance in the proving phase. Our intuition was that guessed linear relations often contain coefficients that are powers of two. Modulo (pseudo) Mersenne primes, such coefficients map to small residues, which could simplify the SAT-based verification. To test this conjecture, we compared the default configuration of TALISMAN2.0 using only pseudo Mersenne primes in the range $2^{16} \pm 50$ with a configuration using randomly selected primes from the interval $[2^{15}, 2^{17}]$. The latter exhibited only a negligible average slowdown of 1.2%, indicating that the choice of primes has little practical impact.

7 Conclusion & Future Work

We presented a hybrid multimodular framework for word-level verification of arithmetic circuits that completely avoids arbitrary-precision arithmetic. By performing algebraic reasoning in parallel over word-sized prime fields and combining linear with nonlinear rewriting, our approach achieves both efficiency and robustness. Our implementation in TALISMAN2.0 shows that this design significantly improves performance in practice.

An important next step is the integration of proof logging techniques such as [23, 24] into our framework. In particular, recycling proof steps as proposed in [24] appears especially promising in the multimodular setting. We also plan to investigate methods for generating short proofs of ideal membership [16]. Beyond circuit verification, we expect that our techniques can be applied also to related problems such as equivalence checking.

Acknowledgments. C.H. was supported by the LIT AI Lab funded by the state of Upper Austria and by the Austrian Science Fund (FWF) [10.55776/COE12]. D.K. was supported by the Austrian Science Fund (FWF) under grant [10.55776/ESP666].

Disclosure of Interests. The authors have no competing interests to declare that are relevant to the content of this article.

References

1. Arnold, E.A.: Modular algorithms for computing Gröbner bases. *Journal of Symbolic Computation* **35**(4), 403–419 (2003)
2. Berkeley Logic Synthesis and Verification Group: ABC: A System for Sequential Synthesis and Verification. <http://www.eecs.berkeley.edu/~alanmi/abc/> (2019), bitbucket Version 1.01
3. Biere, A., Faller, T., Fazekas, K., Fleury, M., Froleyks, N., Pollitt, F.: CaDiCaL 2.0. In: Proc. of the 36th International Conference on Computer Aided Verification (CAV) 2024, Part I. *Lecture Notes in Computer Science*, vol. 14681, pp. 133–152. Springer (2024). https://doi.org/10.1007/978-3-031-65627-9_7
4. Brown, W.S.: On Euclid’s algorithm and the computation of polynomial greatest common divisors. *Journal of the ACM* **18**(4), 478–504 (1971)
5. Buchberger, B.: Ein Algorithmus zum Auffinden der Basiselemente des Restklassenringes nach einem nulldimensionalen Polynomideal. Ph.D. thesis, University of Innsbruck (1965)
6. Cox, D.A., Little, J., O’Shea, D.: *Ideals, Varieties, and Algorithms – an Introduction to Computational Algebraic Geometry and Commutative Algebra*. Undergraduate texts in mathematics, Springer, 2nd edn. (1997)
7. Cox, D.A., Little, J., O’Shea, D.: *Using Algebraic Geometry*. Springer (2005)
8. Gerhard, J., Von zur Gathen, J.: *Modern Computer Algebra*. Cambridge University Press, 3rd edn. (2013)
9. GMP: The GNU Multiple Precision Arithmetic Library, <https://gmplib.org>
10. Golia, P., Soos, M., Chakraborty, S., Meel, K.S.: Designing Samplers is Easy: The Boon of Testers. In: Proc. of 2021 Formal Methods in Computer Aided Design (FMCAD). pp. 222–230 (2021). https://doi.org/10.34727/2021/isbn.978-3-85448-046-4_31
11. Heisinger, M., Hofstadler, C.: f4ncgb: High Performance Gröbner Basis Computations in Free Algebras. In: Proc. of the International Workshop on Computer Algebra in Scientific Computing (CASC) 2025. pp. 79–97. Springer (2025)
12. Hofstadler, C., Kaufmann, D.: TalisMan. <https://doi.org/10.4230/artifacts.23376>, <https://github.com/d-kfmnn/talisman/tree/be8187d>, software, version 1.0., swbId: swb:1:dir:8af022a61661d2b7fb281abbd2f18d51f221c20 (visited on 2025-08-08)
13. Hofstadler, C., Kaufmann, D.: Guess and Prove: A Hybrid Approach to Linear Polynomial Recovery in Circuit Verification. In: Proc. of the 31st International Conference on Principles and Practice of Constraint Programming (CP) 2025. *Leibniz International Proceedings in Informatics (LIPIcs)*, vol. 340, pp. 14:1–14:22 (2025). <https://doi.org/10.4230/LIPIcs.CP.2025.14>
14. Hofstadler, C., Kaufmann, D., Chen, C.: TalisMan2.0 - Artifact. <https://tucloud.tuwien.ac.at/index.php/s/FyfjHm4iWCZwT9T> (2026), will be moved to a permanent online repository upon acceptance
15. Hofstadler, C., Levandovskyy, V.: Modular Algorithms for Computing Gröbner Bases in Free Algebras. arXiv preprint arXiv:2502.11606 (2025)
16. Hofstadler, C., Verron, T.: Short proofs of ideal membership. *Journal of Symbolic Computation* **125**, 102325 (2024)
17. Homma, N., Watanabe, Y., Aoki, T., Higuchi, T.: Formal design of arithmetic circuits based on arithmetic description language. *IEICE Trans. Fundam. Electron. Commun. Comput. Sci.* **89-A**(12), 3500–3509 (2006). <https://doi.org/10.1093/ietfec/e89-a.12.3500>

18. Kaufmann, D., Beame, P., Biere, A., Nordström, J.: Adding Dual Variables to Algebraic Reasoning for Gate-Level Multiplier Verification. In: Proc. of 2022 Design, Automation & Test in Europe Conf. & Exhibition (DATE). pp. 1431–1436. IEEE (2022). <https://doi.org/10.23919/DATE54114.2022.9774587>
19. Kaufmann, D., Berthomieu, J.: Extracting Linear Relations from Gröbner Bases for Formal Verification of And-Inverter Graphs. In: Proc. of Tools and Algorithms for the Construction and Analysis of Systems (TACAS). vol. 15696, pp. 355–374. Springer (2025). https://doi.org/10.1007/978-3-031-90643-5_19
20. Kaufmann, D., Biere, A.: AMulet 2.0 for Verifying Multiplier Circuits. In: Proc. of Tools and Algorithms for the Construction and Analysis of Systems (TACAS). LNCS, vol. 12652, pp. 357–364. Springer (2021). https://doi.org/10.1007/978-3-030-72013-1_19
21. Kaufmann, D., Biere, A., Kauers, M.: Verifying Large Multipliers by Combining SAT and Computer Algebra. In: Proc. of Formal Methods in Computer Aided Design (FMCAD). pp. 28–36. IEEE (2019). <https://doi.org/10.23919/FMCAD.2019.8894250>
22. Kaufmann, D., Biere, A., Kauers, M.: Incremental column-wise verification of arithmetic circuits using computer algebra. *Formal Methods Syst. Des.* **56**(1), 22–54 (2020). <https://doi.org/10.1007/s10703-018-00329-2>
23. Kaufmann, D., Fleury, M., Biere, A., Kauers, M.: Practical algebraic calculus and Nullstellensatz with the checkers Pacheck and Pastèque and Nuss-Checker. *Formal Methods in System Design* **64**(1), 73–107 (2024). <https://doi.org/10.1007/s10703-022-00391-x>
24. Kaufmann, D., Hofstadler, C.: Recycling Algebraic Proof Certificates. In: Proc. of the 10th International Workshop on Satisfiability Checking and Symbolic Computation (SC-Square) 2025. vol. 4116, pp. 35–40. Ceur (2025), <https://ceur-ws.org/Vol-4116/>
25. Konrad, A., Scholl, C.: FastPoly: An Efficient Polynomial Package for the Verification of Integer Arithmetic Circuits. In: Proc. of Formal Methods in Computer Aided Design (FMCAD). pp. 139–144 (2024). https://doi.org/10.34727/2025/isbn.978-3-85448-084-6_20
26. Konrad, A., Scholl, C.: Symbolic Computer Algebra for Multipliers Revisited - It’s All About Orders and Phases. In: Proc. of Formal Methods in Computer-Aided Design (FMCAD). pp. 261–271. IEEE (2024). https://doi.org/10.34727/2024/isbn.978-3-85448-065-5_32
27. Konrad, A., Scholl, C., Mahzoon, A., Große, D., Drechsler, R.: Divider Verification Using Symbolic Computer Algebra and Delayed Don’t Care Optimization. In: Proc. of Formal Methods in Computer-Aided Design (FMCAD). pp. 1–10. IEEE (2022). https://doi.org/10.34727/2022/isbn.978-3-85448-053-2_17
28. Kuehlmann, A., Paruthi, V., Krohm, F., Ganai, M.K.: Robust Boolean reasoning for equivalence checking and functional property verification. *IEEE Trans. Comput. Aided Des. Integr. Circuits Syst.* **21**(12), 1377–1394 (2002). <https://doi.org/10.1109/TCAD.2002.804386>
29. Mahzoon, A., Große, D., Drechsler, R.: PolyCleaner: clean your polynomials before backward rewriting to verify million-gate multipliers. In: Proc. of Intl. Conf. on Computer-Aided Design (ICCAD). p. 129. ACM (2018). <https://doi.org/10.1145/3240765.3240837>
30. Mahzoon, A., Große, D., Scholl, C., Drechsler, R.: Towards Formal Verification of Optimized and Industrial Multipliers. In: Proc. of Design, Automation & Test in Europe Conf. & Exhibition (DATE). pp. 544–549. IEEE (2020). <https://doi.org/10.23919/DATE48585.2020.9116485>

31. Mayr, E.W., Meyer, A.R.: The complexity of the word problems for commutative semigroups and polynomial ideals. *Advances in mathematics* **46**(3), 305–329 (1982)
32. Monagan, M., Pearce, R.: A compact parallel implementation of F4. In: *Proc. of the 2015 International Workshop on Parallel Symbolic Computation*. pp. 95–100 (2015)
33. Philipp, T., Steinke, P.: PBLib - A Library for Encoding Pseudo-Boolean Constraints into CNF. In: *Proc. of 18th Intl. Conf. on Theory and Applications of Satisfiability Testing (SAT) 2015*. LNCS, vol. 9340, pp. 9–16. Springer (2015). https://doi.org/10.1007/978-3-319-24318-4_2
34. Stein, W.A.: *Modular Forms: A Computational Approach*, vol. 79. American Mathematical Soc. (2007)
35. The FLINT team: FLINT: Fast Library for Number Theory (2025), version 3.4.0, <https://flintlib.org>

A Benchmark Details

The components of the *aoki*-benchmarks are:

- PPG: simple (sp), Booth encoding radix-4 (bp);
- PPA: Array (ar), Wallace tree (wt), Balanced delay tree (bd), Overturned-stairs tree (os), Dadda tree (dt), (4;2) compressor tree (ct), (7,3) counter tree (cn), Red. binary addition tree (ba);
- FSA: Ripple-carry (rc), Carry look-ahead (cl), Ripple-block carry look-ahead (rb), Block carry look-ahead (bc), Ladner-Fischer (lf), Kogge-Stone (ks), Brent-Kung (bk), Han-Carlson (hc), Conditional sum (cn), Carry select (cs), Carry-skip fix size (csf), Carry-skip var. size (csv)

All of these circuits have an input bit-width of 64 and consist of 38 000 to 52 000 nodes.

B Experimental Data

Table 2: Per-phase runtime (rounded to tenths of seconds) of TALISMAN2.0. In columns marked with ‘*’ we report the average time per prime modulus. Entries ‘-’ indicate that this phase was not entered.

Name	Total	TALISMAN2.0 — Phase Times (s)								
		Linear							Nonlinear	
		Prepr.	Extract	Sample	Guess*	Prove*	Repair*	Rewrite	Simplify	Rewrite
bp-ar-bc	5.2	1.5	0.7	0.1	1.1	1.3	-	0.1	<0.05	0.2
bp-ar-bk	4.7	1.5	0.5	0.1	1.0	1.1	-	0.1	<0.05	0.2
bp-ar-cl	44.0	1.4	0.7	0.9	9.7	26.6	3.0	0.1	<0.05	0.2
bp-ar-cn	48.0	1.6	<0.05	2.3	26.7	3.2	12.8	<0.05	0.4	0.3
bp-ar-cs	8.4	1.5	<0.05	0.7	4.2	1.2	-	<0.05	0.2	0.1
bp-ar-csf	4.4	1.5	0.4	0.1	0.7	1.2	-	0.1	<0.05	0.2
bp-ar-csv	4.5	1.5	0.5	0.1	0.7	1.2	-	0.1	<0.05	0.2
bp-ar-hc	5.5	1.5	0.4	0.2	1.9	0.9	-	0.1	<0.05	0.2
bp-ar-ks	8.0	1.5	0.5	0.3	4.1	1.1	-	0.1	<0.05	0.2
bp-ar-lf	5.3	1.4	0.5	0.1	1.6	1.0	-	0.1	<0.05	0.2
bp-ar-rb	5.2	1.5	0.5	0.2	1.4	1.2	-	0.1	<0.05	0.2
bp-ar-rc	4.7	1.5	0.4	0.1	0.9	1.1	-	0.1	<0.05	0.2
bp-ba-bc	5.7	1.5	0.5	0.2	1.7	1.4	-	0.1	<0.05	0.2
bp-ba-bk	6.1	1.4	0.5	0.2	2.1	1.2	-	0.1	<0.05	0.2
bp-ba-cl	104.0	1.5	1.0	1.9	26.3	61.3	9.6	0.2	<0.05	0.2
bp-ba-cn	42.0	1.6	<0.05	2.3	23.0	3.6	5.3	<0.05	4.8	0.4
bp-ba-cs	13.5	1.6	<0.05	1.3	8.0	1.6	-	<0.05	0.4	0.1
bp-ba-csf	5.1	1.5	0.5	0.1	1.0	1.3	-	0.1	<0.05	0.2
bp-ba-csv	5.0	1.5	0.5	0.1	1.0	1.3	-	0.1	<0.05	0.2
bp-ba-hc	8.8	1.5	0.6	0.3	4.4	1.4	-	0.1	<0.05	0.2
bp-ba-ks	27.6	1.5	1.0	2.0	15.8	5.6	0.2	0.1	<0.05	0.2
bp-ba-lf	9.8	1.5	0.5	0.3	4.3	1.4	1.1	0.1	<0.05	0.2
bp-ba-rb	7.1	1.5	0.5	0.2	2.5	1.3	-	0.1	<0.05	0.2
bp-ba-rc	5.2	1.5	0.5	0.2	1.2	1.3	-	0.1	<0.05	0.2
bp-bd-bc	5.2	1.4	0.5	0.2	1.4	1.2	-	0.1	<0.05	0.2
bp-bd-bk	5.2	1.4	0.5	0.1	1.5	1.1	-	0.1	<0.05	0.2

Table 2: Per-phase runtime (rounded to tenths of seconds) of TALISMAN2.0. In columns marked with ‘*’ we report the average time per prime modulus. Entries ‘-’ indicate that this phase was not entered.

Name	Total	TALISMAN2.0 — Phase Times (s)								
		Linear							Nonlinear	
		Prepr.	Extract	Sample	Guess*	Prove*	Repair*	Rewrite	Simplify	Rewrite
bp-bd-cl	86.2	1.4	0.9	1.6	21.6	50.1	8.3	0.2	<0.05	0.2
bp-bd-cn	24.4	1.5	0.1	1.6	11.3	5.9	0.9	<0.05	1.9	0.4
bp-bd-cs	30.3	1.5	0.5	3.2	22.2	1.9	-	0.1	<0.05	0.2
bp-bd-csf	4.8	1.4	0.5	0.1	1.0	1.3	-	0.1	<0.05	0.2
bp-bd-csv	4.8	1.4	0.5	0.1	1.0	1.3	-	0.1	<0.05	0.2
bp-bd-hc	6.9	1.4	0.5	0.2	3.1	1.1	-	0.1	<0.05	0.2
bp-bd-ks	12.3	1.4	0.5	0.6	7.3	1.9	-	0.1	<0.05	0.2
bp-bd-lf	6.6	1.4	0.5	0.2	2.7	1.3	-	0.1	<0.05	0.2
bp-bd-rb	6.1	1.4	0.5	0.2	2.2	1.2	-	0.1	<0.05	0.2
bp-bd-rc	5.2	1.4	0.7	0.2	1.2	1.2	-	0.1	<0.05	0.2
bp-cn-bc	9.4	1.4	1.2	0.2	2.8	2.8	-	0.1	<0.05	0.2
bp-cn-bk	8.9	1.4	1.2	0.2	2.8	2.5	-	0.1	<0.05	0.2
bp-cn-cl	104.5	1.4	3.0	1.9	27.7	58.5	9.0	0.3	<0.05	0.2
bp-cn-cn	31.3	1.5	<0.05	1.9	19.1	4.0	2.7	<0.05	0.4	0.6
bp-cn-cs	13.5	1.5	<0.05	1.4	7.9	1.6	-	<0.05	0.2	0.4
bp-cn-csf	11.1	1.4	2.3	0.1	3.4	2.9	-	0.2	<0.05	0.2
bp-cn-csv	11.3	1.4	2.3	0.2	3.5	3.0	-	0.2	<0.05	0.2
bp-cn-hc	14.2	1.4	2.2	0.3	6.3	2.9	-	0.2	<0.05	0.2
bp-cn-ks	20.3	1.4	2.3	0.8	11.0	3.7	-	0.2	<0.05	0.2
bp-cn-lf	13.9	1.4	2.3	0.3	5.8	3.0	-	0.2	<0.05	0.2
bp-cn-rb	12.9	1.4	2.2	0.3	5.0	3.0	-	0.2	<0.05	0.2
bp-cn-rc	11.6	1.4	2.2	0.2	3.8	2.9	-	0.2	<0.05	0.2
bp-ct-bc	7.2	0.9	2.1	0.2	2.1	1.2	-	0.1	<0.05	0.2
bp-ct-bk	7.0	0.9	2.1	0.2	2.1	1.1	-	0.1	<0.05	0.2
bp-ct-cl	88.6	0.9	2.8	1.7	22.7	48.5	8.8	0.2	<0.05	0.2
bp-ct-cn	18.8	1.0	<0.05	1.1	8.9	3.1	0.9	<0.05	2.6	0.4
bp-ct-cs	12.1	1.0	<0.05	1.3	7.4	1.5	-	<0.05	0.2	0.2
bp-ct-csf	6.6	0.9	2.1	0.1	1.6	1.2	-	0.1	<0.05	0.2
bp-ct-csv	6.6	1.0	2.1	0.1	1.6	1.2	-	0.1	<0.05	0.2
bp-ct-hc	9.0	0.9	2.1	0.2	3.9	1.1	-	0.1	<0.05	0.2
bp-ct-ks	14.6	0.9	2.1	0.7	8.3	1.8	-	0.1	<0.05	0.2
bp-ct-lf	8.7	0.9	2.1	0.2	3.5	1.3	-	0.1	<0.05	0.2
bp-ct-rb	8.1	0.9	2.2	0.2	2.9	1.2	-	0.1	<0.05	0.2
bp-ct-rc	6.8	1.0	2.2	0.2	1.8	1.1	-	0.1	<0.05	0.2
bp-dt-bc	5.4	1.3	0.5	0.2	1.6	1.3	-	0.1	<0.05	0.2
bp-dt-bk	5.2	1.3	0.5	0.2	1.6	1.2	-	0.1	<0.05	0.2
bp-dt-cl	98.6	1.4	1.4	1.9	25.4	56.8	8.9	0.2	<0.05	0.2
bp-dt-cn	34.4	1.4	<0.05	2.2	22.0	3.7	3.3	<0.05	0.4	0.4
bp-dt-cs	13.1	1.4	<0.05	1.3	8.0	1.7	-	<0.05	0.2	0.1
bp-dt-csf	4.7	1.3	0.5	0.1	1.0	1.3	-	0.1	<0.05	0.2
bp-dt-csv	4.8	1.3	0.5	0.1	1.0	1.3	-	0.1	<0.05	0.2
bp-dt-hc	7.5	1.3	0.5	0.3	3.6	1.2	-	0.1	<0.05	0.2
bp-dt-ks	13.6	1.2	0.5	0.7	8.5	2.0	-	0.1	<0.05	0.2
bp-dt-lf	7.1	1.3	0.5	0.2	3.3	1.3	-	0.1	<0.05	0.2
bp-dt-rb	5.4	1.3	0.5	0.2	1.6	1.3	-	0.1	<0.05	0.2
bp-dt-rc	4.9	1.3	0.5	0.2	1.2	1.2	-	0.1	<0.05	0.2
bp-os-bc	5.3	1.4	0.5	0.2	1.5	1.2	-	0.1	<0.05	0.2
bp-os-bk	5.3	1.4	0.4	0.2	1.6	1.2	-	0.1	<0.05	0.2
bp-os-cl	88.2	1.4	0.9	1.6	21.9	52.1	8.0	0.2	<0.05	0.2
bp-os-cn	21.2	1.5	0.1	1.5	9.8	5.8	0.7	<0.05	0.8	0.4

Table 2: Per-phase runtime (rounded to tenths of seconds) of TALISMAN2.0. In columns marked with ‘*’ we report the average time per prime modulus. Entries ‘-’ indicate that this phase was not entered.

Name	Total	TALISMAN2.0 — Phase Times (s)								
		Linear							Nonlinear	
		Prepr.	Extract	Sample	Guess*	Prove*	Repair*	Rewrite	Simplify	Rewrite
bp-os-cs	12.6	1.5	<0.05	1.2	7.3	1.7	-	<0.05	0.3	0.1
bp-os-csf	4.8	1.4	0.5	0.1	1.0	1.3	-	0.1	<0.05	0.2
bp-os-csv	4.9	1.4	0.5	0.1	1.0	1.3	-	0.1	<0.05	0.2
bp-os-hc	7.3	1.4	0.5	0.3	3.5	1.1	-	0.1	<0.05	0.2
bp-os-ks	12.9	1.4	0.5	0.6	7.7	2.0	-	0.1	<0.05	0.2
bp-os-lf	7.7	1.4	0.5	0.2	2.9	1.3	0.7	0.1	<0.05	0.2
bp-os-rb	6.5	1.4	0.5	0.2	2.4	1.3	-	0.1	<0.05	0.2
bp-os-rc	5.4	1.4	0.8	0.2	1.3	1.2	-	0.1	<0.05	0.2
bp-wt-bc	5.2	1.4	0.5	0.1	1.4	1.3	-	0.1	<0.05	0.2
bp-wt-bk	5.2	1.4	0.5	0.1	1.4	1.1	-	0.1	<0.05	0.2
bp-wt-cl	81.5	1.4	0.9	1.6	20.4	47.9	6.9	0.1	<0.05	0.2
bp-wt-cn	21.3	1.5	0.1	1.4	8.7	5.3	0.6	<0.05	2.7	0.4
bp-wt-cs	11.9	1.5	<0.05	1.1	6.8	1.5	-	<0.05	0.3	0.1
bp-wt-csf	4.8	1.4	0.5	0.1	0.9	1.3	-	0.1	<0.05	0.2
bp-wt-csv	4.8	1.4	0.5	0.1	0.9	1.3	-	0.1	<0.05	0.2
bp-wt-hc	7.1	1.4	0.5	0.2	3.1	1.3	-	0.1	<0.05	0.2
bp-wt-ks	11.9	1.4	0.5	0.6	7.2	1.6	-	0.1	<0.05	0.2
bp-wt-lf	6.6	1.4	0.5	0.2	2.6	1.3	-	0.1	<0.05	0.2
bp-wt-rb	6.1	1.4	0.5	0.2	2.2	1.2	-	0.1	<0.05	0.2
bp-wt-rc	4.8	1.4	0.5	0.1	1.1	1.2	-	0.1	<0.05	0.2
sp-ar-bc	4.2	2.2	<0.05	0.1	0.4	1.2	-	<0.05	-	-
sp-ar-bk	3.9	2.1	<0.05	0.1	0.4	1.1	-	<0.05	-	-
sp-ar-cl	19.7	2.2	0.1	0.4	3.1	12.6	0.6	0.1	-	-
sp-ar-cn	10.0	2.2	<0.05	0.5	4.2	1.6	0.7	<0.05	0.3	0.1
sp-ar-cs	4.3	2.2	<0.05	0.2	1.1	0.7	-	<0.05	-	-
sp-ar-csf	4.1	2.2	<0.05	<0.05	0.3	1.4	-	<0.05	-	-
sp-ar-csv	4.2	2.2	<0.05	0.1	0.3	1.4	-	<0.05	-	-
sp-ar-hc	4.3	2.1	<0.05	0.1	0.7	1.0	-	<0.05	-	-
sp-ar-ks	4.6	2.1	<0.05	0.1	1.3	0.8	-	<0.05	-	-
sp-ar-lf	4.2	2.1	<0.05	0.1	0.7	1.0	-	<0.05	-	-
sp-ar-rb	4.2	2.1	<0.05	0.1	0.6	1.1	-	<0.05	-	-
sp-ar-rc	2.4	2.2	<0.05	<0.05	<0.05	<0.05	-	<0.05	-	-
sp-ba-bc	6.1	2.5	0.1	0.1	1.4	1.6	-	0.1	-	-
sp-ba-bk	6.4	2.5	0.1	0.2	1.9	1.4	-	0.1	-	-
sp-ba-cl	110.1	2.6	0.5	1.8	25.0	68.1	10.1	0.1	-	-
sp-ba-cn	48.6	2.7	0.1	2.8	25.0	7.1	2.8	<0.05	6.7	0.3
sp-ba-cs	14.4	2.7	<0.05	1.3	7.8	1.8	-	<0.05	0.3	0.1
sp-ba-csf	5.6	2.5	0.2	0.1	0.9	1.6	-	0.1	-	-
sp-ba-csv	5.6	2.5	0.2	0.1	0.9	1.6	-	0.1	-	-
sp-ba-hc	9.0	2.6	0.1	0.3	4.3	1.4	-	0.1	-	-
sp-ba-ks	27.4	2.5	0.3	1.8	15.1	6.4	0.2	0.1	-	-
sp-ba-lf	9.0	2.5	0.1	0.3	4.1	1.6	-	0.1	-	-
sp-ba-rb	7.1	2.5	0.1	0.2	2.4	1.5	-	0.1	-	-
sp-ba-rc	5.6	2.6	0.1	0.2	1.0	1.5	-	0.1	-	-
sp-bd-bc	5.3	2.3	<0.05	0.1	1.2	1.4	-	0.1	-	-
sp-bd-bk	5.2	2.3	<0.05	0.1	1.2	1.3	-	0.1	-	-
sp-bd-cl	88.1	2.3	0.3	1.6	19.8	54.4	7.0	0.2	-	-
sp-bd-cn	23.2	2.4	0.1	1.5	10.1	7.0	0.7	<0.05	0.4	0.3
sp-bd-cs	12.8	2.4	<0.05	1.1	6.7	1.7	-	<0.05	0.3	0.1
sp-bd-csf	4.9	2.3	<0.05	0.1	0.7	1.5	-	<0.05	-	-

Table 2: Per-phase runtime (rounded to tenths of seconds) of TALISMAN2.0. In columns marked with ‘*’ we report the average time per prime modulus. Entries ‘-’ indicate that this phase was not entered.

Name	Total	TALISMAN2.0 — Phase Times (s)								
		Linear						Nonlinear		
		Prepr.	Extract	Sample	Guess*	Prove*	Repair*	Rewrite	Simplify	Rewrite
sp-bd-csv	5.0	2.3	<0.05	0.1	0.8	1.6	-	0.1	-	-
sp-bd-hc	6.8	2.3	<0.05	0.2	2.9	1.0	-	0.1	-	-
sp-bd-ks	11.7	2.3	<0.05	0.6	6.7	1.7	-	0.1	-	-
sp-bd-lf	6.5	2.3	<0.05	0.2	2.4	1.4	-	0.1	-	-
sp-bd-rb	6.2	2.3	<0.05	0.2	1.9	1.4	-	0.1	-	-
sp-bd-rc	5.0	2.3	<0.05	0.1	0.9	1.4	-	<0.05	-	-
sp-cn-bc	22.2	2.7	4.2	0.3	6.7	6.8	-	0.3	-	-
sp-cn-bk	23.2	2.7	4.3	0.3	7.4	6.8	-	0.3	-	-
sp-cn-cl	124.3	2.6	5.3	1.9	30.5	71.7	9.0	0.4	-	-
sp-cn-cn	83.3	2.7	0.1	4.5	53.1	7.1	6.9	<0.05	0.4	6.9
sp-cn-cs	21.4	2.7	<0.05	1.3	7.9	1.8	-	<0.05	0.3	6.8
sp-cn-csf	21.9	2.6	4.4	0.2	6.1	6.9	-	0.3	-	-
sp-cn-csv	22.3	2.6	4.2	0.2	6.4	7.3	-	0.3	-	-
sp-cn-hc	24.2	2.7	4.3	0.4	8.6	6.6	-	0.3	-	-
sp-cn-ks	30.5	2.6	4.2	0.8	13.5	7.7	-	0.3	-	-
sp-cn-lf	24.9	2.6	4.2	0.3	8.4	7.2	-	0.3	-	-
sp-cn-rb	23.6	2.6	4.3	0.3	7.8	6.9	-	0.3	-	-
sp-cn-rc	22.4	2.7	4.2	0.3	6.4	7.0	-	0.3	-	-
sp-ct-bc	10.0	1.7	4.2	0.2	2.2	1.4	-	0.2	-	-
sp-ct-bk	9.6	1.6	4.0	0.2	2.2	1.2	-	0.2	-	-
sp-ct-cl	95.2	1.7	5.2	1.7	22.7	53.6	8.1	0.3	-	-
sp-ct-cn	19.8	1.8	0.1	1.4	8.6	6.1	0.5	<0.05	0.4	0.4
sp-ct-cs	35.1	1.8	4.1	3.2	23.0	1.9	-	0.2	-	-
sp-ct-csf	9.4	1.7	4.2	0.1	1.7	1.4	-	0.2	-	-
sp-ct-csv	9.2	1.6	4.2	0.1	1.5	1.4	-	0.2	-	-
sp-ct-hc	11.9	1.6	4.2	0.2	4.1	1.3	-	0.2	-	-
sp-ct-ks	17.2	1.7	4.1	0.6	8.3	2.0	-	0.2	-	-
sp-ct-lf	11.5	1.7	4.2	0.2	3.5	1.4	-	0.2	-	-
sp-ct-rb	10.8	1.6	4.1	0.2	3.1	1.4	-	0.2	-	-
sp-ct-rc	9.6	1.7	4.2	0.1	1.9	1.3	-	0.2	-	-
sp-dt-bc	5.4	2.2	<0.05	0.2	1.4	1.4	-	0.1	-	-
sp-dt-bk	5.2	2.2	<0.05	0.2	1.3	1.3	-	0.1	-	-
sp-dt-cl	106.3	2.1	0.4	1.7	24.8	65.5	9.5	0.1	-	-
sp-dt-cn	33.3	2.2	0.1	2.5	18.3	7.0	1.5	<0.05	0.4	0.3
sp-dt-cs	32.5	2.3	<0.05	3.4	23.9	2.0	-	0.1	-	-
sp-dt-csf	4.8	2.1	<0.05	0.1	0.8	1.6	-	<0.05	-	-
sp-dt-csv	4.9	2.2	<0.05	0.1	0.8	1.5	-	0.1	-	-
sp-dt-hc	7.2	2.2	<0.05	0.3	3.3	1.2	-	0.1	-	-
sp-dt-ks	13.3	2.1	<0.05	0.7	8.0	2.1	-	0.1	-	-
sp-dt-lf	6.8	2.1	<0.05	0.2	2.8	1.4	-	0.1	-	-
sp-dt-rb	6.4	2.2	<0.05	0.2	2.3	1.4	-	0.1	-	-
sp-dt-rc	2.3	2.1	<0.05	<0.05	<0.05	<0.05	-	<0.05	-	-
sp-os-bc	6.4	2.3	<0.05	0.1	1.3	1.7	-	0.1	-	-
sp-os-bk	5.4	2.3	<0.05	0.1	1.3	1.4	-	0.1	-	-
sp-os-cl	101.0	2.3	0.4	1.8	22.9	61.7	9.5	0.2	-	-
sp-os-cn	25.3	2.4	0.1	1.7	11.5	7.2	0.7	<0.05	0.4	0.3
sp-os-cs	13.7	2.5	<0.05	1.2	7.4	1.8	-	<0.05	0.3	0.1
sp-os-csf	5.0	2.3	<0.05	0.1	0.8	1.6	-	0.1	-	-
sp-os-csv	5.1	2.3	<0.05	0.1	0.8	1.6	-	0.1	-	-
sp-os-hc	7.2	2.3	<0.05	0.3	3.1	1.2	-	0.1	-	-

Table 2: Per-phase runtime (rounded to tenths of seconds) of TALISMAN2.0. In columns marked with ‘*’ we report the average time per prime modulus. Entries ‘-’ indicate that this phase was not entered.

Name	Total	TALISMAN2.0 — Phase Times (s)								
		Linear						Nonlinear		
		Prepr.	Extract	Sample	Guess*	Prove*	Repair*	Rewrite	Simplify	Rewrite
sp-os-ks	12.9	2.3	<0.05	0.6	7.6	2.0	-	0.1	-	-
sp-os-lf	7.0	2.3	<0.05	0.2	2.7	1.5	-	0.1	-	-
sp-os-rb	6.7	2.4	<0.05	0.2	2.2	1.5	-	0.1	-	-
sp-os-rc	5.2	2.3	<0.05	0.2	1.0	1.4	-	<0.05	-	-
sp-wt-bc	5.5	2.3	<0.05	0.2	1.2	1.5	-	0.1	-	-
sp-wt-bk	5.2	2.3	<0.05	0.2	1.2	1.3	-	0.1	-	-
sp-wt-cl	85.3	2.3	0.3	1.5	18.8	52.6	6.7	0.1	-	-
sp-wt-cn	19.2	2.4	0.1	1.1	6.9	7.0	0.4	<0.05	0.4	0.3
sp-wt-cs	12.5	2.4	<0.05	1.1	6.6	1.7	-	<0.05	0.3	0.1
sp-wt-csf	5.0	2.3	<0.05	0.1	0.7	1.5	-	0.1	-	-
sp-wt-csv	5.0	2.3	<0.05	0.1	0.7	1.5	-	0.1	-	-
sp-wt-hc	6.9	2.3	<0.05	0.2	2.8	1.2	-	0.1	-	-
sp-wt-ks	11.7	2.3	<0.05	0.6	6.6	1.8	-	0.1	-	-
sp-wt-lf	6.5	2.3	<0.05	0.2	2.3	1.4	-	0.1	-	-
sp-wt-rb	6.2	2.3	<0.05	0.2	1.9	1.4	-	0.1	-	-
sp-wt-rc	5.0	2.3	<0.05	0.2	0.9	1.4	-	0.1	-	-
abc32-cmp	0.3	0.3	<0.05	<0.05	<0.05	<0.05	-	<0.05	-	-
abc32-dc2	0.2	0.2	<0.05	<0.05	<0.05	<0.05	-	<0.05	-	-
abc32-resyn	0.2	0.2	<0.05	<0.05	<0.05	<0.05	-	<0.05	-	-
abc32-resyn2	0.2	0.2	<0.05	<0.05	<0.05	<0.05	-	<0.05	-	-
abc32-resyn3	0.2	0.2	<0.05	<0.05	<0.05	<0.05	-	<0.05	-	-
abc64-cmp	2.3	2.1	<0.05	<0.05	<0.05	<0.05	-	<0.05	-	-
abc64-dc2	2.3	2.1	<0.05	<0.05	<0.05	<0.05	-	<0.05	-	-
abc64-resyn	2.3	2.1	<0.05	<0.05	<0.05	<0.05	-	<0.05	-	-
abc64-resyn2	2.3	2.1	<0.05	<0.05	<0.05	<0.05	-	<0.05	-	-
abc64-resyn3	2.3	2.2	<0.05	<0.05	<0.05	<0.05	-	<0.05	-	-
abc128-cmp	34.0	32.6	<0.05	<0.05	<0.05	<0.05	-	0.1	-	-
abc128-dc2	33.4	32.0	<0.05	<0.05	<0.05	<0.05	-	0.1	-	-
abc128-resyn	33.5	32.0	<0.05	<0.05	<0.05	<0.05	-	0.1	-	-
abc128-resyn2	34.5	33.0	<0.05	<0.05	<0.05	<0.05	-	0.1	-	-
abc128-resyn3	33.8	32.4	<0.05	<0.05	<0.05	<0.05	-	0.1	-	-